arXiv:0709.1139v2 [astro-ph] 9 Sep 2007

Cosmic String Detection via Microlensing of Stars

David F. Chernoff [1] **and S.-H. Henry Tye** [2]

[1]Department of Astronomy
Cornell University, Ithaca, NY 14853

[2]Newman Laboratory for Elementary Particle Physics
Cornell University, Ithaca, NY 14853

ABSTRACT: Cosmic superstrings are produced towards the end of the brane inflation, a scenario realized in modern superstring theory. If the string tension is low enough, loops tend to be relatively long-lived. The resultant string network is expected to contain many loops which are smaller than typical Galactic scales. Cosmic expansion damps the center of mass motion of the loops which then cluster like cold dark matter, eventually decaying by emission of gravitational radiation.

Loops will lens stars within the galaxy and local group. We explore microlensing of stars as a tool to detect and to characterize some of the fundamental string and string network properties, including the dimensionless string tension $G\mu/c^2$ and the density of string loops within the Galaxy.

As $G\mu \to 0$ the intrinsic microlensing rate diverges as $1/\sqrt{G\mu}$ but experimental detection will be limited by shortness of the lensing timescale and/or smallness of the bending angle which each vary $\propto G\mu$. We find that detection is feasible for a range of tensions. As an illustration, the planned optical astrometric survey mission, Gaia, should be able to detect numerous microlensing events for string networks with tensions $10^{-10} \lesssim G\mu \lesssim 10^{-6}$. A null result for optical microlensing implies $G\mu \lesssim 10^{-10}$.

If lensing of a given source *is* observed it will repeat because the internal motions of the loop are relativistic but the center of mass motion may be much smaller, of order the halo velocity v_h. This distinctive hallmark, $c/v_h \sim 1000$ repetitions, suggests a useful method for confirmation of a potential lensing detection.

We argue that the estimate of the Galactic lensing frequency is likely to rise with more realistic descriptions of the superstring network while the effect of the inclusion of loop-loop interactions within the Galactic halo is not yet clear.

KEYWORDS: Cosmic strings, string theory, cosmology, inflationary universe, brane world, brane inflation.

Contents

1. Introduction

Inflation probably explains the origin of our universe [1]. A concrete realization of this scenario in superstring theory is brane inflation [2, 3, 4]. The simplest version involves an interacting D3-$\overline{\text{D}}$3-brane system in which the D3-brane moves towards the $\overline{\text{D}}$3-brane sitting at the bottom of a warped throat, with the position of the mobile D3-brane corresponding to the inflaton. Inflation ends when the D3-brane and the $\overline{\text{D}}$3-brane collide and annihilate, initiating the hot big bang. Cosmic strings are copiously produced during the epoch of annihilation [5, 6]. These strings are simply superstrings (F- and D-strings and their bound states [7, 8, 9]) stretched to cosmological sizes. Finding evidence for the existence of these strings would go a long way towards confirming certain fundamental aspects of superstring theory [10, 11].

The single most important property of a cosmic string is its tension μ, or, in dimensionless terms, the characteristic gravitational potential $G\mu/c^2$ [12] (hereafter, we will take $c = 1$). An initial estimate of the range of tension produced towards the end of inflation gave $10^{-11} \lesssim G\mu \lesssim 10^{-6}$ [6]. A recent analysis of the reheating that accompanies brane inflation, including multi-brane multi-throat scenarios, suggests that $G\mu < 10^{-11}$

is quite possible [13]. The properties of the cosmic superstrings produced at the end of inflation are compatible with all observations today but are beginning to be constrained by observational data [14, 15, 16]. The actual bound is sensitive to the details of the string tension spectrum and the probability of string-string interactions but $G\mu \lesssim 10^{-7}$ gives a rough idea of current observational constraints.

For small $G\mu$, it will be very challenging to detect cosmic string signatures in lensing, gravitational wave bursts, pulsar timing and B mode polarization in the cosmic microwave background radiation by methods that have been investigated hitherto. However, even low $G\mu$ strings produce double images of point-like objects. Here, we will investigate the utility of microlensing of stars to learn about the string content of the universe. The propensity to microlens depends, of course, upon the number of lenses and their cross section for bending light. Our current understanding of string network evolution implies that the rate of lensing increases as $G\mu$ decreases. This happy circumstance may eventually lead to practical experiments to detect superstrings. Microlensing of stars is much more promising than microlensing of quasars [17].

Although it is well accepted that cosmic strings evolve to a scaling network [18], string network evolution is by no means well understood. Even if one had a complete knowledge of the intrinsic string tensions in string theory, the cosmological evolution of the string network remains a challenging problem [11]. Recent analyses strongly suggest that cosmic superstrings evolve dynamically so as to produce a scaling solution in which there exists a stable relative distribution of strings with different quantum numbers [19, 20]. This is very much like the behavior of cosmic strings generated by abelian Higgs or Nambu-Goto type models [18, 12]. The superstring solutions found in current string theory, however, form a much larger class which is only now being explored.

A scaling solution implies the fractions of the critical energy density in long strings and loops are constant. In fact, the determination of Ω_{long} and Ω_{loop} has been an outstanding question for some time [12]. Numerical simulations for cosmic strings may be fitted by

$$\Omega_s \equiv \Omega_{long} + \Omega_{loop} = \psi G\mu + \chi \sqrt{G\mu} \qquad (1.1)$$

for constants ψ and χ. A small isolated loop of length l will decay in a characteristic time $\tau = l/(\Gamma G\mu)$ and $\Gamma \sim 50$ for Nambu-Goto strings. A common assumption made in many simulations is that small loops are produced by the intersection of long strings (including self intersection). For $H\tau << 1$ where H is the Hubble constant the loops decay quickly via gravitational radiation and $\Omega_s \sim \Omega_{long} \sim \psi G\mu$; the loop contribution is negligible. Numerical simulations show $\psi \sim \Gamma$. Presumably, this is a good approximation for $G\mu$ close to the present day observational bound.

Several new considerations have emerged from the latest simulations and from theoretical work.

- Loops dominate: For small $G\mu$ newly formed loops do not immediately dissipate. The latest simulations [21, 25, 24] imply a loop distribution which, if truncated by

gravitational wave damping, yields a qualitatively new effect: $\Omega_s \sim \Omega_{loop} >> \Omega_{long}$.

- Small scales on long strings: Analytic work [29, 11] shows that the stretching of long strings is insufficient to prevent the development of small scale structure. Collisions of long strings may produce large numbers of loops of all sizes. Estimates indicate $\sim 10\%$ of the long string length ends up in loops with scale comparable to the horizon. Loops with $H\tau \gtrsim 1$ contribute to Ω_s.

- Backreaction of small scales: When Ω_{loop} increases, small loops can recombine to form bigger loops and, likewise, isolated loops may be incorporated into long strings. The determination of the scaling solution when energy can flow up and down a hierarchy of scales is an outstanding problem.

- Damping of loops vs long strings: Analytic work [26, 27] indicates that the rate of damping of modes on long strings differs from $\Gamma G\mu$, the characteristic loss rate for an isolated loop. Under such circumstances the network- and time-averaged gravitational energy loss rate per mode is coupled to the details of the intercommutation process.

These factors motivate the development of a very approximate description of the string network when the tension is low. Specifically, we extend the analysis of Olum et al. in Ref.[21] to describe the loop population for small $G\mu$. We also parameterize the effective decay rate of loops in the network by $\Gamma_R G\mu$ where, in general, we expect $\Gamma_R < \Gamma \sim 50$.

This minimal quantitative framework is used to begin an investigation of microlensing by loops. Lensing by cosmic string loops at cosmological distances was considered originally in [31, 32]. The analyses focused on $G\mu \sim 10^{-6}$ and the possibility that the lensing might produce multiple images of QSOs. The situation of interest here is quite different though the physical process, gravitational lensing, remains the same as was originally discussed in these papers. We shall first give a brief sketch of the latest status of the cosmic string network. We shall outline the form of the loop distribution which is presented in full detail in the Appendix. We shall then use the result to estimate the event rates and the detectability of microlensing for the cosmic strings. While many properties of superstrings and astrophysics remain unaccounted for (specifically, the intercommutation probability and the collisional interactions within the Galaxy) this approach highlights the role of lowering $G\mu$ and sets a benchmark that we will refine as the input physics is better understood.

Our analysis shows that the intrinsic rate of microlensing increases as tension decreases. At the same time the detection efficiency for a microlensing event diminishes because both the duration of the event and also the size of the deficit angle diminish.[1]

---

[1]The deficit angle due to the string must be bigger than the angle subtended by a star. For typical

To illustrate the potential utility for detecting cosmic string microlensing of stars, we consider the upcoming European Gaia mission [22]. Gaia is primarily an astrometry satellite designed to measure proper motions and parallaxes of about 10^9 stars in and near the Galaxy over a 5 year period. The satellite records the flux for each star and it is this feature which is of greatest interest to us. On average each star will be observed 80 times; individual observations take about ~ 3 seconds. The expected accuracy of the photometry from a single observation is easily sufficient to see a factor of 2 change in flux from one observation to the next. Using a crude model of detection efficiency, *we find that an instrument like Gaia would be able to detect microlensing events for cosmic strings in the Galaxy: a few events for $G\mu \sim 10^{-10}$ to a few dozens for $G\mu \sim 10^{-8}$.* This estimate invokes several conservative choices including the value of Γ_R; the event rate increases for $\Gamma_R < \Gamma$.

A key reason for this detectable rate is the over-density of loops in the Galaxy. Even small loops can survive a Hubble time when the tension is low. A generally new scenario for cosmic string evolution now unfolds: the velocity of the center of mass of a loop decreases on account of cosmic drag; loop-loop interactions freeze out. Loops subsequently behave like cold dark matter, slowly radiating gravitational waves. Most of the loops of interest for microlensing were born during the radiation era and fall into gravitational perturbations that begin to grow after equipartition. In particular, the loops track the perturbations of the cold dark matter. This clumping enhances the local loop density by at least a factor of $\sim 10^5$.

From the string theory point of view, the true lensing rate may be *enhanced* above our estimate because the intercommutation probability of superstrings may be as small as $P \sim 10^{-3}$ [19]. Also, cosmic superstrings come in a variety of tensions and charges so that a number of species are present in the network [20]. These effects will tend to increase the energy density throughout the universe in the superstring network in eq. (1.1) roughly like $\Omega_s \to n\Omega_s/P$, where n is the effective number of types, $n \sim 5$. The spectrum of cosmic superstrings yields a discrete set of tensions that can easily vary by an order of magnitude.

From an astrophysical point of view, the true lensing rate may be *enhanced* by dissipative loop-halo interactions that boost the galactic loop density and it may be *diminished* by the collisional interaction of loops once they begin to clump in the Galaxy. Intercommutation might chop up small loops into smaller loops and shorten their lifetime to gravitational wave emission. This, in turn, may diminish the part of the spectrum responsible for most of the lensing while increasing the locally generated gravitational

---

sources (a solar mass main sequence star within the halo) this is roughly $G\mu \gtrsim 10^{-14}$. Likewise, the duration δt_{lens} of the shortest detectable optical microlensing event is limited by, among other things, the ability to detect a factor of 2 change in the number of the source photons. If we assume a typical source (a solar mass star at distance 10 kpc), a broadband instrument detecting photons near the peak of the spectrum (~ 1 eV), a typical instrument (a 10% efficient meter-class telescope), then we can estimate that a 5σ detection requires $\delta t_{lens} \gtrsim 40$ ms. This corresponds to roughly $G\mu \gtrsim 10^{-14}$.

wave background. We have not included either the dissipation or the interaction in our microlensing estimates but will return to these issues in the future.

2. String Network

We shall start by considering cosmological cosmic strings like Nambu-Goto strings or vortices in an abelian Higgs model. One readily identifies two components, long horizon-crossing segments and sub-horizon closed loops. Only straight strings are static; all others are dynamic with relativistic motion. Even isolated loops oscillate in a highly complicated fashion. A network of long strings and loops can change topology by the process of intercommutation, the breaking and rejoining experienced when the motions of two segments of string cause them to coincide in 3D space. This process can fragment as well as rejoin the basic elements of the string network. Self intersections of a long string cuts off new loops, self intersections of a loop transforms it to multiple loops, etc. Conversely, inverse processes allow loops to reconnect to long strings and loops to reconnect with other loops. In the cosmological context the processes of intercommutation, damping (e.g. gravitational wave emission) and cosmological expansion govern the string network evolution.

When a network exhibits scaling behavior the energy density (either long or loop) is a fixed fraction of the critical energy density eq. (1.1). When very small loops are formed and decay promptly the critical density

$$\Omega_s \sim \Omega_{long} \sim \psi G\mu \tag{2.1}$$

and simulations show $\psi \sim \Gamma$ where $\Gamma \sim 50$ for abelian strings. The scaling solution depends upon Γ in an indirect way. Small scale structure on the long strings is damped by gravitational wave emission with rate $\propto \Gamma G\mu$ if one assumes modes damp like those of an isolated loop. An intersection of two long string segments is more dissipative if it converts a greater overall length to small loops. In fact, more loops are produced if the segment possesses more small scale structure. The dissipation per collision of long string segments, therefore, scales $\propto 1/\Gamma G\mu$. The rate for one segment of a horizon-crossing string to encounter another $\propto \Omega_{long}$. Therefore, the total dissipation rate per long string segment $\propto \Omega_{long}/\Gamma G\mu$. A fixed rate of dissipation per string is essential to achieve a scaling solution in the first place, so that $\Omega_{long} \propto \Gamma G\mu$.

The specific scenario above depends on the $H\tau << 1$ where H is the Hubble constant, $\tau = l/\Gamma G\mu$ is the damping time and l is the loop size. In a scaling solution a typical loop formed at time t has size $l \sim \alpha t$ where α is constant so $\alpha/\Gamma G\mu << 1$ is required. The value of α is poorly known; $\alpha < 10^{-12}$ is sometimes invoked [12] but recent numerical simulations [23, 28] and analytic studies [29] suggest that loops with a range of sizes $10^{-4} \lesssim \alpha \lesssim 0.25$ are created. Lower tension implies longer damping time so that the prompt loop decay which is characteristic of the scenario above is now more difficult to achieve.

To build a model capable of describing the loop distribution for small $G\mu$ we follow the line of reasoning of Olum et al. [21]. In the radiation or matter-dominated eras the number of loops produced per unit loop length per unit volume per unit time has the form

$$\frac{dN(l,t)}{dl\,dt\,dV} = t^{-5}f(x) \qquad \text{with } x = l/t \tag{2.2}$$

for some function $f(x)$ for a scaling solution.[2] Numerical simulation in Ref.[23, 28] suggest a power law distribution of loops

$$f(x) = Ax^{-\beta} \qquad \text{for } x < \alpha \tag{2.3}$$

where αt is the largest loop scale and $\beta < 2$. The constants A, α and β may be extracted from time-dependent simulations for cosmic strings which appear to have entered a scaling regime.

Assume that in each infinitesimal time interval $(t, t + dt)$ the network produces the loops described with $l < \alpha t$ according to $dN/dl\,dt\,dV$ and these are subsequently diluted by cosmological expansion without further intercommutation. This is an instantaneous fragmentation description adjusted to agree with the results of time-dependent simulations that model the complete process. A non-interacting loop shrinks by gravitational wave emission until it disappears in time $l/(\Gamma_R G\mu)$. Note the introduction of Γ_R in the dimensionless decay rate in place of $\Gamma \sim 50$. Here, $\Gamma_R < \Gamma$ implies that loops live longer because of complex unmodeled network effects. For example, in the conventional view, a loop of size l emits energy at half the total rate of two loops of size $l/2$. In addition, [26, 27] find that the damping rate of long strings is $\propto (G\mu)^k$ with $k > 1$. For the simple energy loss recipes employed it makes a great deal of difference whether a length is part of a small loop, a large loop or a long, horizon-crossing string. We do not attempt to disentangle these effects but simply introduce Γ_R as an effective damping rate.

The superstrings differ from previously studied cosmic strings in fundamental characteristics like $G\mu$ and P and possibly in the resultant loop distribution described by A, α and β. It is tricky to extrapolate to describe domains not previously simulated. Our calculation of the distribution function for loops is given in detail in Appendix 1. The general idea is as follows: When the network scales the long strings are chopped to loops whose total length is a constant fraction of the horizon. Energy conservation implies that $\int fx\,dx$ is fixed. If the typical loop size α were to be modified (for example, because the intercommutation probability is decreased), then this energy conservation argument gives $A \propto \alpha^{\beta-2}$. Using this reasoning we can, in principle, consider various descriptions for f, cosmological expansion dynamics, Γ_R and $G\mu$. The minimal assumption is that $(1 - \langle v^2 \rangle)/\gamma_s^2$ is the same for undamped Nambu-Goto strings in Minkowski space as for damped superstring networks in FRW cosmology; here, the characteristic inter-string

---

[2]This form does not apply during the recent, Λ-dominated phase since the horizon is not $\propto t$. The loops of direct interest to us are from earlier epochs.

distance $d(t) = \gamma_s t$ and $\langle v^2 \rangle$ is the square of the string velocity averaged over the length of long strings. For our applications, however, we also assume the simulation-derived quantities like β are fixed and concentrate on changes to the network that arise from varying $G\mu$, Γ_R and the cosmological dynamics.

At any time the distribution of non-interacting loops in a given volume is the integrated production rate over the history of the universe

$$\frac{dN}{dl\,dV} = \frac{1}{V} \int \frac{dN}{dl\,dV\,dt'} V(t') dt' \tag{2.4}$$

subject to upper and lower cutoffs. The upper cutoff corresponds to the time when gravitational wave damping removes the loop; the lower cutoff is the earliest epoch when the loop might be produced. If the expansion scale factor varies $a \propto t^n$ then the integrand $\propto t^{3n+\beta-5}$. For both radiation and matter dominated eras, the loop distribution at length l is typically dominated by production at early times $t = l/\alpha$ (this requires $\beta < 7/2$ or 3, respectively) so that

$$\frac{dN}{dl\,dV} \propto \frac{l^{3n-4}}{t^{3n} \alpha^{3n-2}} \tag{2.5}$$

as previously demonstrated by Vanchurin et al. [28]. This distribution may then be compared to the cosmological simulation results [25, 24]. None of the simulations incorporate gravitational damping so that the cutoff at small loop size in the simulations reflects either initial conditions, finite resolution and/or finite simulation times. Nonetheless, the results at various epochs illustrates the buildup of a powerlaw distribution of loops at intermediate scales with the predicted slope. In the radiation era, for example, eq. (2.5) gives $dN/dl\,dV \propto l^{-2.5}$ while the simulations of Ringeval et al. [25] imply $dN/dl\,dV \propto l^{-2.6}$.

The energy density, lensing probability and lensing rate of loops all involve essentially the same moment of the loop distribution, $\int l\,dl \frac{dN}{dl\,dV}$. The cutoff $l = \Gamma_R G\mu t$ is the key parameter which varies with the tension when we evaluate those quantities. For loops originally generated in the radiation era

$$\rho_{loops} \propto \frac{\mu}{t^2} \left(\frac{\alpha}{\Gamma_R \mu} \right)^{1/2} \tag{2.6}$$

Since $\rho_{cr} \propto 1/Gt^2$ we infer

$$\Omega_{loops} \propto \sqrt{\frac{\alpha\mu}{\Gamma_R}} \tag{2.7}$$

This illustrates the combination of parameters that determines Ω_{loop}; if $\Omega_{long} \propto G\mu$ this square-root behavior suggests that $\Omega_{loop} > \Omega_{long}$ for small $G\mu$.

The numerical simulations which include both loops and long strings allow a quantitative check. Assume that the slope and amplitude of the simulation-derived loop distribution is extended to the gravitational cutoff and that the long string density is

fixed. The ratio is

$$\frac{\Omega_{long}}{\Omega_{loop}} = \begin{cases} 4.4 \times 10^{-4} \sqrt{\frac{G\mu}{10^{-10}}} & \text{Olum et al. [21]} \\ 7.5 \times 10^{-4} \left(\frac{G\mu}{10^{-10}}\right)^{0.6} & \text{Ringeval et al. [25]} \end{cases} \tag{2.8}$$

which shows the dominance of the loops. The evaluation of the lensing probability and rate involves the same integrals which depend on the gravitational wave damping cutoff in the same way. When strings have low tension *loops, not horizon crossing strings, are the favored lensing candidates.*

The appendix treats general powerlaw forms for f with upper and lower cutoffs (α_U, α_L) and various slopes (β) and, most significantly, various $G\mu$ and radiation loss rates Γ_R. It gives approximate expressions valid for loops from both radiation and matter epochs. It compares the simple analytic approximations to more realistic Λ-CDM cosmologies. It provides a range of numerical solutions illustrating how the loop distribution varies with μ, Γ_R, β, α_L and α_U.

As mentioned earlier, cosmic superstrings have different properties from cosmic strings. The intercommutation probability of vortices is known to be around unity, $P \simeq 1$, while that of superstrings is rather complicated, but $P \sim g_s^2$ [19], where the string coupling $g_s \sim 1/10$. Also, cosmic superstrings come in a variety of tensions and charges so that a number of species are present in the network [20]. These effects likely increase the energy density in the superstring network compared to its cosmic strings counterpart roughly

$$\Omega_s \to \frac{n}{P}\Omega_s \tag{2.9}$$

where n is the effective number of types, $n \sim 5$. For very small P, it has been argued that $1/P \to 1/P^{2/3}$ [30]. The implication is that the number density of small cosmic superstring loops will be boosted with respect to cosmic strings.

3. Microlensing

Microlensing refers to brightness variations of a background source caused by a changing gravitational field somewhere along the line of sight. The field may be generated by a dark point-like object and the astrophysically anticipated candidates include dim stars, white dwarfs, neutron stars, and black holes. The paths of photons emitted by the source are bent so that the angular area of the source visible to the observer changes. In short, the flux from the source changes. The key point is that one does not have to resolve the source or the lens to observe the change. Lensing distorts a single source image or, if the impact parameter of the photon is within the Einstein radius, lensing creates multiple images. The area within the Einstein radius is quite small so its much more common for magnification of a single image to occur than the creation of multiple images. If source, lens and observer have constant velocities, the time-dependent magnification has

an *a priori* known functional form. Previous surveys (MACHO, OGLE, EROS, etc.) have searched for and identified numerous events with the expected time-dependent achromatic form.

Now, instead of the normal astrophysical lensing candidates, consider a stationary straight infinite string oriented perpendicular to the observer's line of sight with respect to a background source. Let two photons from the source travel toward the string. The photons do not suffer any relative deflection during the fly-by as long as they pass around the string in the same sense. Images formed from photons are undistorted. This contrasts with the shear and distortion produced by a point mass.

However, there is a small angular region just like the Einstein radius that yields multiple images as long as the source itself is small in angular size compared to the Einstein radius. In essence, some of the photons pass around the the string in a clockwise sense and others do so in a counterclockwise sense. Two paths from the source to the observer yield two undistorted images.

Sources that lie behind the string and within the characteristic angle $\sim 8\pi G\mu$ will appear as double images. Unresolved, lensed sources will appear to fluctuate in brightness by a factor of 2 as the angular region associated with the string passes across the observer-source line of sight. The characteristic Einstein angle is

$$\Theta_E = 8\pi G\mu$$
$$= 1.04 \times 10^{-3} \left(\frac{G\mu}{2 \times 10^{-10}} \right) \text{arcsec.} \tag{3.1}$$

The characteristic angular size of a stellar source at distance R is $\Theta_\odot = R_\odot/R$. The relative size is

$$\frac{\Theta_\odot}{\Theta_E} = 4.5 \times 10^{-5} \left(\frac{2 \times 10^{-10}}{G\mu} \right) \left(\frac{100\text{kpc}}{R} \right) \tag{3.2}$$

which shows when the stellar source will generally be well described as a point source. The relativistically moving and oscillating string will create brightness fluctuations in the background star that can be searched for in a microlensing experiment.

The actual situation is somewhat more complicated. For a loop, as opposed to a straight string, one expects lensing like that of a point mass for photons with impact parameter large compared to the size of the loop and lensing like that of a straight string for paths that pass close to a segment of the string. We will eschew the complications associated with small scale structure on the string and concentrate on photons that pass close to a smooth segment of the loop.

The characteristic scale of the smallest loops today is

$$l_g = \Gamma_R G\mu t_{today} = 41\text{pc} \left(\frac{\Gamma_R G\mu}{10^{-8}} \right) \left(\frac{t_{today}}{13.5\text{Gyr}} \right). \tag{3.3}$$

and the characteristic mass scale associated with such a loop is

$$M_g = 1.7 \times 10^5 \text{M}_\odot \left(\frac{G\mu}{2 \times 10^{-10}} \right)^2 \left(\frac{\Gamma_R}{50} \right) \tag{3.4}$$

both of which are small compared to Galactic scales.

For comparison, the characteristic scale of the loops formed at equipartition is

$$l_{max,eq} = \alpha_U t_{eq} = \alpha_U 14\text{kpc} \left(\frac{t_{eq}}{4.7 \times 10^4 \text{yrs}} \right). \tag{3.5}$$

Galactic scales are $R \sim 1 - 100$ kpc and microlensing can probe the full range of loops generated during the radiation era plus the small end of the loops generated during the matter era. All this assumes α_U order unity. Generally, the internal velocities associated with loops are relativistic.

We want to answer two questions: What is the probability for lensing a single source at distance R by a distribution of loops at a given instant? How does the probability grow with time?

Consider a small loop of size l at distance r. It lenses an angular area $\Omega_L \sim (\theta_E r)l/r^2$. The probability that a single background source at distance R is lensed is the ratio of the lensed angular area to the observed angular area in the direction of the source. We find

$$P_L = \int r^2 dr \int \mathcal{F} \frac{dN}{dV dl} \frac{\theta_E l}{r} dl \tag{3.6}$$

and $\mathcal{F}$ is the overdensity of loops in the Galaxy ($\mathcal{F} = 1$ gives the lensing probability in a uniform Universe. We will estimate $\mathcal{F}$ below.) Assuming the ordering $l_g < l_{max,eq} < R < \alpha_U t_{today}$ we find for a homogeneous loop distribution

$$P_L = 3.4 \times 10^{-15} \mathcal{F} \left(\frac{G\mu}{2 \times 10^{-10}} \right) \left(\frac{R}{100\text{kpc}} \right)^2 \left(\frac{1.35 \times 10^{10}\text{yrs}}{t_{today}} \right)^2 H(x, y) \tag{3.7}$$

where H is the first moment of the loop distribution scaled to fiducial parameters. This approximate analytic result is based on two joined powerlaws for radiation and matter eras. In the appendix we show

$$H(x, y) = (0.63 + 0.37\sqrt{y} + 0.04 \log x) \tag{3.8}$$

$$x = \left(\frac{\alpha_U}{0.3} \right) \left(\frac{10^{-8}}{\Gamma_R G\mu} \right) \tag{3.9}$$

$$y = x \left(\frac{t_{eq}}{4.7 \times 10^4 \text{yrs}} \right) \left(\frac{1.35 \times 10^{10}\text{yrs}}{t_{today}} \right) \tag{3.10}$$

Note that as $\Gamma_R G\mu \to 0$ that H varies. In particular, $x \propto y \propto 1/\Gamma_R G\mu$ and $P_L \propto \sqrt{\mu/\Gamma_R}$. Extending the loop distribution to smaller sizes ($\mu \to 0$), therefore, does not overcome the effect of the decrease in Einstein radius.

A numerical evaluation of P_L in the Λ-CDM model is presented in Figure 1 for the basic parameter space in $G\mu - \Gamma_R$ we will consider. The string network has $\alpha_U = 0.3$, $\alpha_L = 10^{-4}$, $\beta = 1.6$ with normalization set by agreement with simulations $\Upsilon = 43.6$ (see Appendix). Here and elsewhere the numerical results we present are based on the
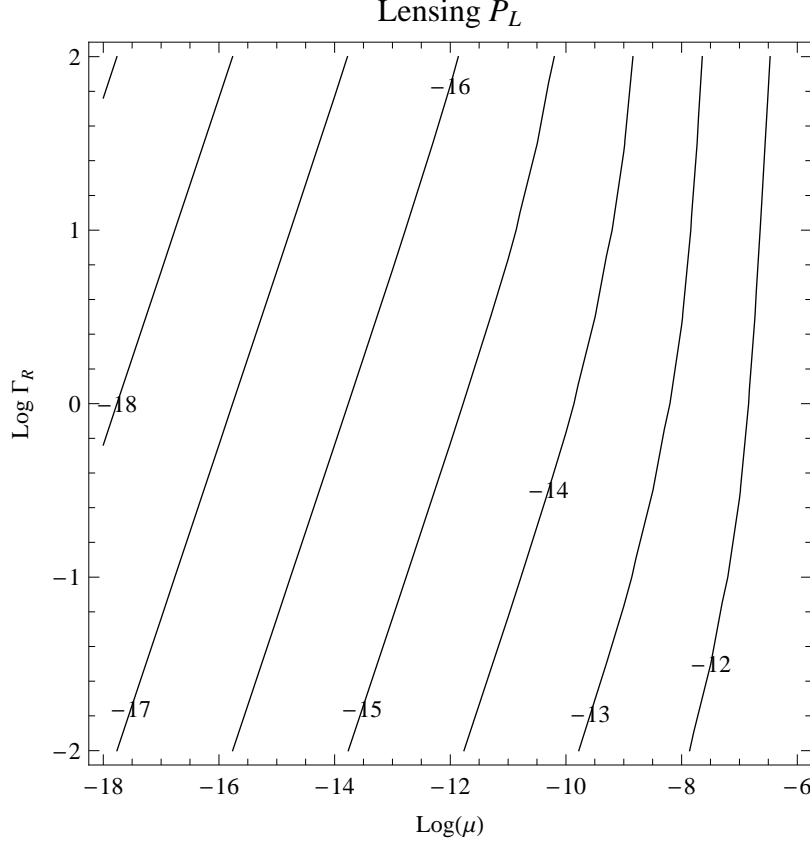
Figure 1: Probability that a line of sight to a source at $R = 100$ kpc is microlensed by intervening string loops in a homogeneous Universe ($\mathcal{F} = 1$).

fiducial Λ-CDM cosmology; the approximate analytic results illustrate the basic scalings.

Now consider an experiment that stares at a given source and looks for the doubling in brightness on account of the passage of a loop along the line of sight. One loop sweeps out an area per unit time $\sim cl/\sqrt{3}$ where the numerical factor crudely accounts for velocity orientation effects. The rate of change in the solid angle is $d\Omega_L/dt \sim cl/\sqrt{3}r^2$. The lensing rate is

$$R_L = \int r^2 dr \int \mathcal{F}\frac{dN}{dV\,dl}\frac{cl}{\sqrt{3}r^2}dl \tag{3.11}$$

which yields the lensing rate per source per year for a homogeneous loop distribution

$$R_L = 2.3 \times 10^{-12}\mathcal{F}\left(\frac{R}{100\text{kpc}}\right)\left(\frac{1.35 \times 10^{10}\text{yrs}}{t_{today}}\right)^2 H(x,y). \tag{3.12}$$

By contrast to the situation for P_L, when $\Gamma_R G\mu \to 0$ we find $R_L \propto \sqrt{1/\Gamma_R\mu}$.

The numerical evaluation of R_L for the same Λ-CDM model as described above is shown in Figure 2.

We have estimated the rate R_L assuming that the loop is moving relativistically. This is generally the case for the internal motions of the loop about its center of mass.
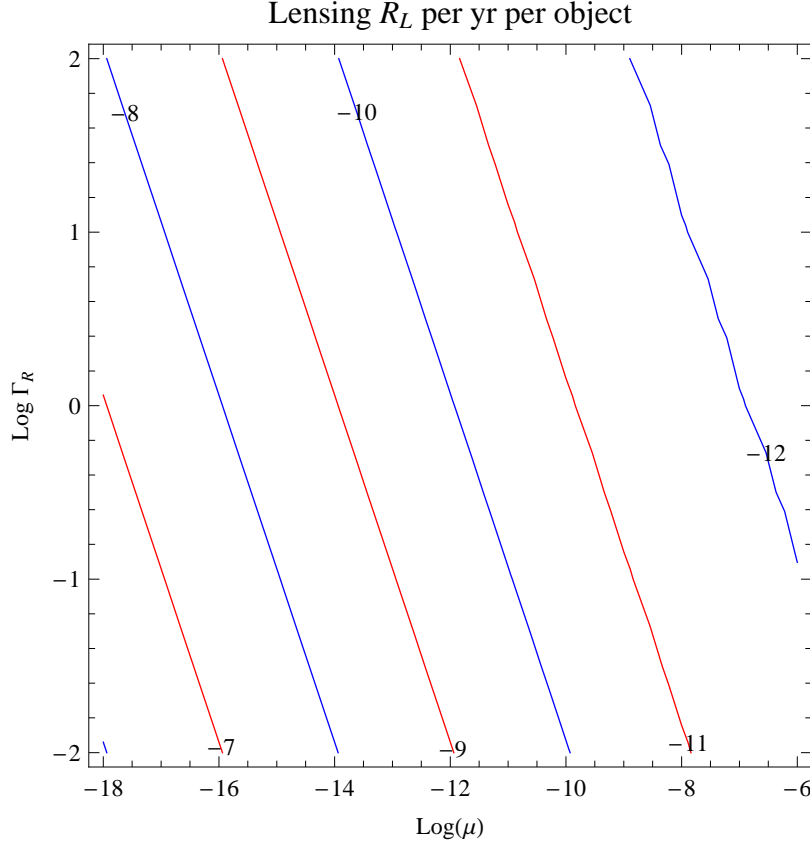
Figure 2: Rate of microlensing along a line of sight to a source at $R = 100$ kpc by intervening string loops in a homogeneous Universe ($\mathcal{F} = 1$).

The velocity of the center of mass of a loop accreted to the Galaxy will be the halo velocity v_h as we describe in more detail in the next section. New sources are lensed at a rate $(v_h/c)R_L$ with repetition $\sim c/v_h$.

4. Cosmology of Small $G\mu$ Loops

The *center of mass velocity* of string loops within the galaxy is a key parameter in characterizing the lensing rate for two reasons. First, if the velocity is less than the characteristic escape velocity from the Galaxy v_h then loops will accrete and be bound to the halo. Second, if the velocity of small loops is much less than c then a single source is lensed multiple times.

The initial loop velocity is determined by the interactions in the string network. Intercommutations between string segments can generate relativistic center of mass motions for the newly formed loops. Our treatment of the loop distribution is based on the assumption that all intercommutations occurs shortly after a horizon-crossing loop is chopped up. General scaling arguments suggest that the interaction rate diminishes

rapidly. Without interactions, the center of mass velocity suffers cosmic drag.[3]

Assume that the initial center of mass velocity is $v_{ci} = 0.1c$ at time t_i when the loop is born. At later time t the center of mass velocity is [35]

$$v_c(t) = \frac{v_{ci}x}{\sqrt{1 - v_{ci}^2 + v_{ci}^2 x^2}} \tag{4.1}$$

$$x = \frac{a(t_i)}{a(t)} \tag{4.2}$$

Figure 3 shows the fraction f_{slow} of the first moment of $dN/dV\,dl$ attributed to slow moving objects. "Slow" means the loop's center of mass velocity today < 300 km s^{-1} in the Λ-CDM model with the fiducial parameters. The first moment is dominated by
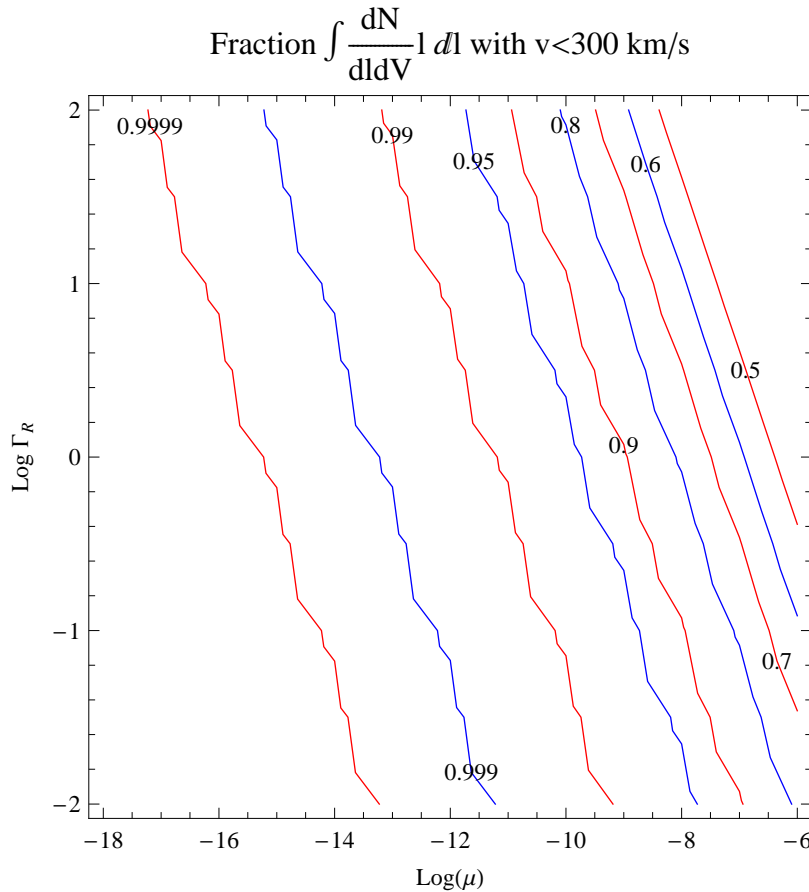
Figure 3: The fraction of the length-weighted loop density distribution with center of mass velocity < 300 km $^{-1}$.

objects moving slowly enough to bind to the current halo.

The scale of the gravitational potential induced by a low tension string is small compared to that of the amplitude of perturbations entering the horizon $\sim 10^{-5}$. At

---

[3]We assume that the recoil from emitted gravitational wave radiation is small.

equipartition $\Omega_{loop} \sim 0.0016\sqrt{G\mu/2 \times 10^{-10}}$ and the mass scale of the loop component which contributes most to Ω at that epoch is small ($\sim 0.5 M_\odot \left(\frac{G\mu}{2\times10^{-10}}\right)^2$). We first treat the low tension strings as "test particles" with respect to the baryons and CDM perturbations. As the perturbations begin to collapse after equipartition the slow moving loops fall into the gravitational potentials which will eventually give rise to galaxies.

The observed overdensity of material in the Galaxy is

$$f_{over} = \frac{\rho_{Gal}}{\Omega_M \rho_{crit}} \tag{4.3}$$

$$\sim 1.5 \times 10^5 \tag{4.4}$$

where we have used $\Omega_M = 0.3$, $H_0 = 70$ km s^{-1} Mpc^{-1}, and a galactic mass of $2\times10^{11}M_\odot$ in a characteristic size of 20 kpc [33]. The size scale has been selected in consideration of the location of stars of interest for microlensing. An estimate for the local enhancement of loops is

$$\mathcal{F} = f_{slow} f_{over} \tag{4.5}$$

i.e. roughly the overdensity of the Galaxy itself.

The above estimate for $\mathcal{F}$ is a lower bound because the actual dynamical evolution of the loops is not dissipationless. At equipartition, a loop begins to accrete matter. A novel aspect of the structure formation in this scenario is that suitably small loops will radiate and disappear but leave behind bound sub-galactic clumps of matter. Such objects are of considerable interest in their own right but here we focus on the mass density of the smallest surviving loops of mass M_g in today's Galaxy. Such a loop accretes a mass $\sim (1 + z_{eq})M_g$ with $z_{eq} \sim 3570$ (in the approximation of a flat, matter-dominated cosmology). This bound, composite object lives in the larger-scale growing galactic potential and it will be dragged by dynamical friction towards the center. As an example, consider the case for $G\mu = 2 \times 10^{-10}$, where $M_g \sim 1.7 \times 10^5 M_\odot$ and clump mass $\sim 6.4 \times 10^8 M_\odot$. Let the clump move on a circular orbit in an isothermal halo with rotation velocity 220 km s^{-1}. The radial drift takes it from ~ 36 kpc to 20 kpc over a Hubble time [34]. The net motion with respect to the halo increases the density of such loops within 20 kpc by at least an additional factor ~ 1.8. The net radial drift for a loop of length l scales $\propto (\mu l)^{1/2}$ and the drift for the smallest surviving loop scales $\propto \mu\sqrt{\Gamma_R}$. These dissipational effects mean that loops, like baryons, may be over-concentrated with respect to the dark matter. The effect on the smallest loops is important if $G\mu \gtrsim 10^{-10}$. The distribution of loop size will also be tilted within the Galaxy compared to $dN/dV\,dl$ on account of the dissipative processes.

We make a conservative estimate for $\mathcal{F}$ in our numerical calculations by ignoring these dissipative enhancements to the loop density.

5. Practical Lensing

There are a number of characteristic timescales relevant to experimental detection of

lensing. For the lensing itself, the characteristic duration of the event is

$$
\begin{aligned}
\delta t_{lens} &= \frac{R\theta_E}{c} \\
&= \frac{R 8\pi G\mu}{c} \\
&= 6.3 \times 10^3 \text{sec} \left(\frac{R}{100\text{kpc}}\right) \left(\frac{G\mu}{2 \times 10^{-10}}\right)
\end{aligned}
\tag{5.1}
$$

The characteristic time for the (smallest) loop to oscillate is

$$
t_{osc} \sim \frac{l_g}{c} \sim 135\text{yrs} \left(\frac{\Gamma_R G\mu}{10^{-8}}\right)
\tag{5.2}
$$

and this governs the repetition timescale.

The observational timescales are δt_1, the time for an individual observation, ΔT, the duration of the experiment, and $\delta\Delta T = \Delta T/N_{rep}$, the characteristic interval between observations where N_{rep} is the number of times a star is visited over the course of the experiment.

To make this concrete, we will consider the Gaia mission which will monitor $N_* = 10^9$ stars for $\Delta T = 5$ yrs with fluxes exceeding a mission-defined broad band magnitude $G = 20$. On average, the Broad-band photometer will observe each star $N_{rep} = 80$ times but the interval between observations is not fixed; it will vary from ~ 30 minutes to $\Delta T/N_{rep}$. An individual observation is $\delta t_1 \sim 3.3$ seconds. Let $\delta\Delta T \sim \Delta T_{obs}/N_{rep}$ be the characteristic interval between repeat observations. The mission observes $\sim 10^3$ stars at a time (note $N_* N_{rep} \delta t_1 >> \Delta T$); all astrometric and photometric results for individual stars are derived by detailed analysis of the joint observations.

The accuracy of the photometry depends upon the brightness of the source. The limiting magnitude $G = 20$ corresponds to objects with a range of usual visual magnitudes $V \sim 20 - 25$. Individual observations for sources with $V = 20, 21, 22$ and 23, for example, have relative flux accuracies 2.5%, 5%, 10% and 26% respectively and are more than adequate to see a factor of 2 change due to microlensing at the limiting magnitude.

A star like the Sun (type G2V) will be visible to a limiting magnitude $V = 20.2$ or a distance approximately 12 kpc. To make estimates of the number of lensing events that Gaia is capable of observing we need to account for the distribution of stars and the "efficiencies" with which detections can be made. We assume here that the stars observed by Gaia are uniformly distributed in space and concentrate on the detection efficiency

$$
f_{det} = f_{mag} f_{size} f_{time}
\tag{5.3}
$$

where f_{mag} is the flux limit, f_{size} is the source size cutoff (so that the angular size

$\Theta < \Theta_E$), and f_{time} accounts for sampling in time. We adopt a crude model

$$f_{time} = \begin{cases} 0 & \text{if} \quad \delta t_{lens} < \delta t_1 \\ \frac{\delta t_{lens}}{\delta \Delta T} & \text{if} \quad \delta t_1 < \delta t_{lens} < \delta \Delta T \\ 1 & \text{if} \quad \delta \Delta T < \delta t_{lens} < \Delta T \\ 0 & \text{if} \quad \Delta T < \delta t_{lens} \end{cases} \qquad (5.4)$$

Any lensing event which is shorter than the length of a single observation or longer than the length of the entire experiment cannot be detected; all remaining events longer than the average interval between observations will be seen but only a fraction of events shorter than it will be. The assumption is that the observational intervals are uniformly spread between the shortest and longest periods. A more accurate description of the schedule of observations will readily improve the model for f_{time}. To find the detectable lensing rate, we recalculate R_L with f_{det} to give R_L^{Gaia}. The expected number of events is $N^{Gaia} = R_L^{Gaia} N_* \Delta T$.

The expected number of lensings detectable by Gaia are shown in Figure 4 by red/blue contours. These include all efficiency factors (magnitude, size and time) with each contour labeled by the log of the number of detectable lensings. Note that the expected number of detectable events decreases as $G\mu \to 0$ at fixed Γ_R (for $G\mu < 10^{-8}$), a consequence of decreased detection efficiency for short duration events ($f_{time} \to 0$). The sharp cutoff as $G\mu \sim 10^{-13}$ is where the angular size of the star becomes comparable to the Einstein angle ($f_{size} \to 0$). The number of events depends on the path length (set by the flux limit f_{mag}) and the intrinsic loop density.

To illustrate the important effect of size and time cutoffs, we also display the expected number of lensing events if detections were limited only by flux considerations (green dashed contours). Note that the expected numbers increase as $G\mu \to 0$. These curves give some guidance on how alternative experiments might fare by adjusting N_{rep}, N_* and ΔT.

An experiment with duration $\Delta T < t_{osc}$ will see at most one lensing event. Conversely, if $\Delta T > t_{osc}$ the experiment has the capability of seeing multiple lensing events from the same source. If $G\mu < 7 \times 10^{-12}$ multiple lensing may be observed by Gaia. In any case, a potential lens can be re-observed by other means even after the mission has ended.

The figure has been constructed for a "typical" star within the Galaxy. The objects included in Gaia's catalog will depend on many factors – stellar type, interstellar obscuration, crowding, etc. – and these will alter the effective cutoffs and the number of events. For example, bright halo giants will be visible within approximately 41 kpc (type G0III; radius $\sim 3.3 R_\odot$). Compared to the more numerous G2V class, the lensing rate per star should be ~ 14 times larger on account of longer pathlengths and longer lensing durations. On the other hand, the cutoff at small $G\mu$ will be comparable to G2V because the angular sizes are comparable at the limiting distance.
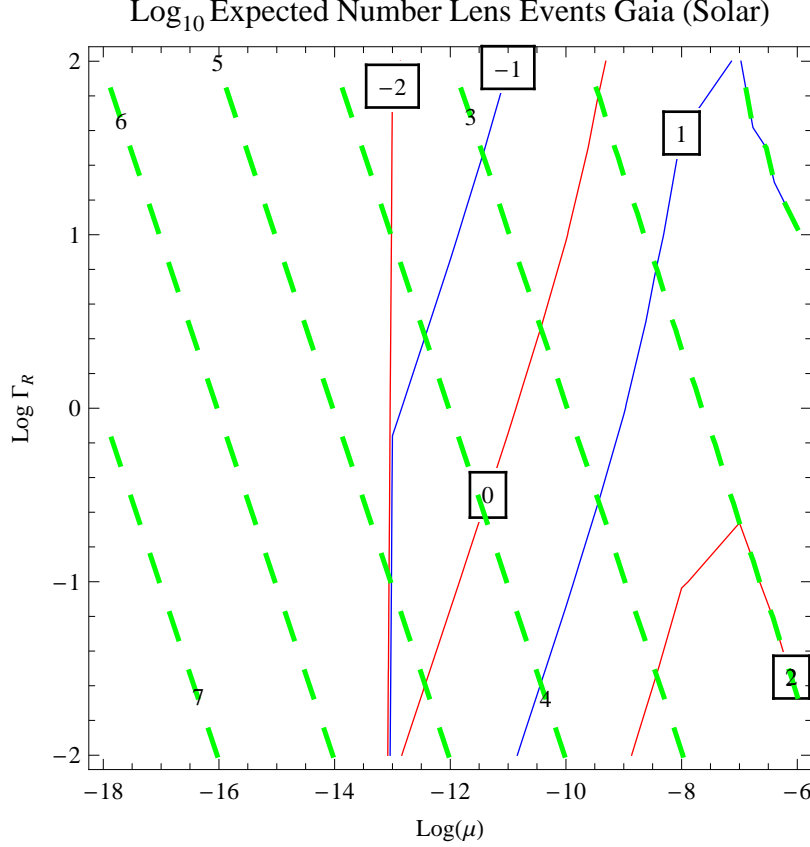
Figure 4: Log of the number of microlensing events detectable by a Gaia-like mission looking at 10^9 sources over 5 years. In this plot all sources are assumed to be solar mass stars (G2V) within 12 kpc. The string loop density is based on the fiducial powerlaw model evolved in a Λ-CDM cosmology. The local string overdensity is $\mathcal{F} = f_{slow} f_{over}$ as described in the text. The red/blue lines include magnitude, time and angular efficiency factors; the dashed green lines include only the flux cutoff.

At the flux limit, a star's angular size $\propto 1/T_{eff}^2$ where T_{eff} is the star's effective temperature. Hotter stars can be seen further and have smaller angular size at the limiting distance. Consequently, the condition that the Einstein angle exceeds the stellar angular size implies a minimum tension detectable by an optical microlensing experiment $\propto 1/T_{eff}^2$. The inclusion of stars hotter than the sun may provide sensitivity to tensions beyond the cutoff indicated in the figure. Of course, the number of such stars is an important consideration: hot white dwarfs, for example, would probe very low tensions but are not visible to large distances. Likewise, the duration of the lensing event should exceed the timescale of a single observation to measure the doubling in image brightness. At the flux limit, the minimum tension $\propto 1/L^{1/2}$ where L is the stellar luminosity. The inclusion of stars more luminous than the sun may provide sensitivity beyond the cutoff. An accurate assessment will depend on the make up of Gaia's catalog, a subject to which we hope to return.

The Broad-band photometer measures 5 colors during an observation but this information is insufficient to allow identification and classification of stellar types throughout the HR diagram; it will be supplemented by photometry in 14 other bands from the Medium-band photometer, a distinct instrument on board. The mission expects to observe $\sim 18 \times 10^6$ variable stars [22] and the extensive color coverage is essential to facilitate identification and classification of known variables types (pulsating stars, eruptive variables, etc.). This circumstance will prove a great benefit if string microlensing is sought. String microlensing is almost achromatic (the Kaiser Stebbins effect gives relative frequency shifts order $\sim G\mu\gamma(v/c)$; since $G\mu$ is small the shift is small for mildly relativistic loop motion) whereas variable stars typically show color changes. The key point is that a cosmic string microlensing event should be an *achromatic* change in brightness by a factor of 2. The situation is qualitatively similar to that faced by ground-based microlensing experiments which anticipate an achromatic change in an *a priori* known form for the time-dependent amplification factor.

Finally, we note that the Broad and Medium-band photometers have their own time sampling characteristics. Depending upon the detailed scheduling of scans, there may be an improved detection efficiency compared to our simple estimate.

6. Remarks

When string tension is low the density in loops exceeds that in long strings because the timescale for gravitational damping becomes long. The total string energy density today is dominated by the loops originally formed during the radiation era. This preponderance of loops over long strings motivates consideration of the cosmology of loops. The evolution of these objects turns out to be completely distinct from that of the long strings originally studied with $G\mu \gtrsim 10^{-6}$.

The loops damp by cosmic drag and are utterly inconsequential in terms of structure formation on scales much larger than the galaxy. Instead, they fall into the potential wells created by cold dark matter and baryons after equipartition. The Galactic halo number density of loops is enhanced over the universe's average value by at least the Galaxy's overdensity $\sim 10^5$. Dissipational effects which depend upon the size of $G\mu$ may further increase the overdensity.

The loops within the Galaxy can be observed by microlensing using stars as sources. To the extent that stars are point-like and bright low tension strings can be observed. Simple estimates of a microlensing survey based on the capabilities of the Gaia mission suggest that many such events may be detected. If loops are moving at halo velocities the lensing of a given source should repeat $\sim 10^3$ times.

Detailed observations of such a lensing source will have much to tell us about string tension and the number density of loops.

We recognize many gaps in this general story

- What processes are responsible for producing the $\mathcal{F} = 1$ (average, unclustered) distribution of loop sizes? When does the rate of interactions between loops and/or long strings become negligible? When does cosmic drag predominate over velocities induced by intercommutation?

- How do loop-loop interactions develop as the galaxy grows? Does intercommutation end up ejecting loops from the galaxy? How does the distribution function of loop sizes change on account of the intercommutations in the dense environment? How small are the smallest loops? Is the gravitational lifetime significantly altered? Can one use this to measure or learn about p? The loop size distribution is potentially measurable via microlensing and locally generated gravitational waves.

- What are the astrophysical constraints on massive loops moving around galaxy? How are loops distributed within the Galaxy?

- What string and loop parameters can we deduce by observing repetitive lensing? Does small scale structure on the loops increase the microlensing repetition rate?

- Incorporate lensing over radii ranging from larger than the loop size to smaller. Is the Kaiser-Stebbins effect detectable from a known lens?

- An accurate calculation of Gaia's capabilities for string microlensing requires in depth analysis of the time-based observing strategy for both the broad and medium band photometers.

- Can one design an experiment tailored to doing a better job for detecting microlensing than a mission like Gaia? It is worth noting that the Gaia sample includes photometry much more accurate than what is needed to detect microlensing. Could one generate a larger catalog with more poorly determined flux measurements still adequate to detect string microlensing? Would there be enough information to rule out variable stars?

- How can one optimize the choice of ΔT, N_{rep} and δt_1 to investigate particular ranges of $G\mu$?

Detecting cosmic superstrings and measuring their tension can reveal fundamental information about superstring theory and elucidate the large-scale contents as well as the remote evolutionary history of our own universe. An observable, nearby source of strings to study promises to advance, qualitatively and quantitatively, these goals.

Acknowledgments

A. Appendix

We start with a form generally consistent with the assumption of a scaling network

$$\frac{dN(l,t)}{dldtdV} = t^{-5}f(x) \qquad \text{with } x = l/t \tag{A.1}$$

where l and V are measured in physical (not comoving) lengths. We make the assumption that the chopping of long strings all the way down to the smallest loops occurs in a time short compared to the expansion timescale. Of course, on the Hubble scale this won't be a very good approximation but it should get better at smaller scales and thats what is of most interest here. Loop length l is the time-averaged physical length associated with the loop when the loop itself is small compared to the scale of the horizon. A cosmological simulation is required to establish the form for f which describes loops with sizes comparable to the scale of the horizon.

Motivated by the numerical simulation in Ref.[23, 28], we take the loop production to be given by a power law distribution with upper and lower cutoffs

$$f(x) = Ax^{-\beta} \qquad \text{for } \alpha_L < x < \alpha_U \tag{A.2}$$

and zero otherwise. In addition to the upper limit, we impose a lower limit on the the range of loops. This is a manifestation of the cutting up process and not due to gravitational wave emission. In this approximate description, dynamical processes chop up strings to give the loop spectrum instantly. Gravitational radiation acts once the spectrum has been created.

The scaling network is characterized by some inter-string distance $d(t) = \gamma_s t$, defined so that the density in long strings is $\rho_\infty = \mu/d^2$. Conservation of energy then gives

$$\int \mu l \frac{dN}{dldVdt}dl = -\frac{d\rho_\infty}{dt} \tag{A.3}$$

or

$$\int_{\alpha_L}^{\alpha_U} xf(x)dx = 2\frac{1}{\gamma_s^2}\left(1 - \langle v^2 \rangle\right) \tag{A.4}$$

where $\langle v^2 \rangle$ is the square of string velocity averaged along the length of long strings.

The energy balance between long strings and the loop distribution gives

$$A = \frac{2\left(1 - \langle v^2 \rangle\right)\left(2 - \beta\right)}{\gamma_s^2 \alpha_U^{2-\beta}\left(1 - (\alpha_L/\alpha_U)^{2-\beta}\right)} \tag{A.5}$$

Numerical simulations [28] derived $A = 82\pm2$, $\alpha_L = 10^{-4}$, $\alpha_U = 10^{-1}$ and $\beta = 1.63\pm0.03$. From these we deduce the numerical value for

$$\Upsilon \equiv \frac{1 - \langle v^2 \rangle}{\gamma_s^2} \simeq 43.6 \tag{A.6}$$

which we will hold fixed even as we consider models with different characteristic values of $G\mu$, α_L, α_U, β and different expansion dynamics $n \neq 2/3$).

It is generally thought that a loop of length l decays by gravitational radiation in time $l/(\Gamma G\mu)$, where Γ is the dimensionless decay rate of order 50. We write our model with two generalizations of the canonical description.

- Γ_R: We introduce a distinct damping rate for loops, Γ_R. It is possible that the average loop damping rate differs substantially from Γ because small loops, large loops and horizon-crossing strings intercommutate.

- τ: Lifetime in the network might be a *nonlinear* function of l. This could arise because of the nontrivial interaction of intercommutation and damping.

If lifetime is linear in length then loops of length l born at time t' and observed at time t must have

$$l > \Gamma_R G\mu(t - t') \qquad \text{for } t > t' \tag{A.7}$$

Our model assumes that loops are unaffected by gravitational wave damping until they reach the end of their life at which point they are abruptly removed from the population.

The loop density at time t_2 due to loops produced during the interval $\mathcal{I} = (t_0, t_1)$ is found by integrating the production rate density production of loops:

$$\frac{dN}{dV dl}(t_2; \mathcal{I}) = \frac{1}{V(t_2)} \int_{t_0}^{t_1} dt' \frac{dN}{dV dl dt'} V(t') \theta(t_2 - t' < \tau(l)) \tag{A.8}$$

Here $V(t)$ is physical volume. Inserting the production rate density

$$\frac{dN}{dV dl}(t_2; \mathcal{I}) = \frac{1}{V(t_2)} \int_{t_0^*}^{t_1^*} dt' \frac{f(\frac{l}{t'})V(t')}{t'^5} \tag{A.9}$$

where

$$t_1^* = \min\left(t_1, \frac{l}{\alpha_L}\right) \tag{A.10}$$

$$t_0^* = \max\left(t_0, t_2 - \tau(l), \frac{l}{\alpha_U}\right). \tag{A.11}$$

A.1 Powerlaw f and $a(t)$

During $\mathcal{I}$ assume that the scale factor $a \propto t^n$, the volume $V \propto t^{3n}$, and $f(x) = Ax^{-\beta}$ for $\alpha_L < x < \alpha_U$ (and 0 otherwise). The loop density at t_2 is

$$\frac{dN}{dVdl}(t_2; \mathcal{I}) = \mathcal{G}\frac{A}{\zeta l^\beta t_2^{3n}(t_0^*)^\zeta}\left(1 - \left[\frac{t_0^*}{t_1^*}\right]^\zeta\right) \tag{A.12}$$

where

$$\zeta = 4 - 3n - \beta. \tag{A.13}$$

For typical values of β and n we have $\zeta > 0$. Now the density at t_2 depends upon how V varies beyond $\mathcal{I}$. If n is constant over the entire interval t_0 to t_2 then $\mathcal{G} = 1$. If loops are born in the radiation-dominated epoch ($n = n_1 = 1/2$), which extends from $t \sim 0$ to $t_{eq} \approx 4.7 \times 10^4$ yrs, and are observed in the matter-dominated and/or lambda-dominated epochs we have a non-trivial $\mathcal{G}$. For the ordering $t_1 < t_{eq} < t_2$, $\mathcal{G} = V_+(t_{eq})t^{3n_1}/V_+(t)t_{eq}^{3n_1}$ where V_+ is the volume for $t > t_{eq}$. If $a(t) \propto t^{n_2}$ for $t > t_{eq}$ then $\mathcal{G} = (t/t_{eq})^{3(n_1-n_2)}$. This reduces to $\mathcal{G} = (t/t_{eq})^{-1/2}$ for $n_1 = 1/2$ and $n_2 = 2/3$.

It will prove useful to rewrite the general result in the following form

$$\frac{dN}{dVdl} = \mathcal{G}\mathcal{N}\frac{\alpha_U^{2-3n}}{l^4}\left(\frac{l}{t}\right)^{3n}\left(\frac{l}{\alpha_U t_0^*}\right)^\zeta\left(1 - \left(\frac{t_0^*}{t_1^*}\right)^\zeta\right) \tag{A.14}$$

$$\mathcal{N} = \frac{2(2-\beta)\Upsilon}{\zeta\left(1 - \left(\frac{\alpha_L}{\alpha_U}\right)^{2-\beta}\right)}. \tag{A.15}$$

Figure 5 presents an estimate of the loop density today obtained by adding the loops created during the radiation and matter-dominated eras. Specifically, we take $n = 1/2$, $t_0 = 0$, $t_1 = t_{eq}$ followed by $n = 2/3$, $t_0 = t_{eq}$, $t_1 = t_2 = t_{today}$. For lack of more precise numbers we take $\alpha_L = 10^{-4}$, $\alpha_U = 0.3$, $\Gamma_R G\mu = \alpha_G = 10^{-8}$ (i.e. lifetime linear in l: $\tau(l) = l/\alpha_G$), $\beta = 1.6$, $\Upsilon = 43.6$ during both epochs. These choices imply $\mathcal{N}_1 = 40$ and $\mathcal{N}_2 = 91$. The background cosmological model has $t_e = 4.7 \times 10^4$ yrs and the current epoch $t_{today} = 1.35 \times 10^{10}$ yrs. The estimate of the number density has a cutoff at $l \simeq 10^{-8}$ from gravitational damping; the very slight kink at loop size $l \simeq 10^{-6}$ is roughly equal to $\alpha_U t_{eq}$ i.e. of order the horizon at equipartition.

Two straight lines are included in the figure and are evidently close approximations to the slope of $dN/dVdl$ over an intermediate regime. The slope is determined by the expansion rate. Assume a pure powerlaw expansion with $t_0 = 0$ and $t_1 = t_{today}$, $\alpha_L \ll \alpha_U$ and $\zeta > 0$ (e.g. $\beta = 1.6$ and $1/2 \leq n \leq 2/3$ gives $0.9 \geq \zeta \geq 0.4$). Define the lengths $l_{min} = \alpha_L t$, $l_{max} = \alpha_U t$ and $l_g = \alpha_G t$. For l large compared to both the gravitational damping and the minimum chopping scales $t_0^* \to \frac{l}{\alpha_U}$ and for l small compared to the horizon $l \ll l_{max}$ we have

$$\frac{dN}{dVdl} = \mathcal{N}\frac{\alpha_U^{2-3n}}{l^4}\left(\frac{l}{t}\right)^{3n} \tag{A.16}$$

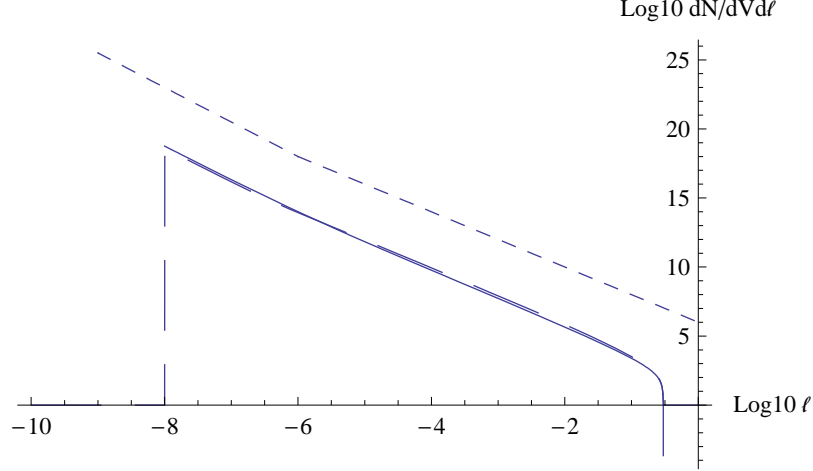**Figure 5:** The number density of today's string distribution based on two powerlaw semi-analytic estimate (long dashs) and ΛCDM model (solid line). Two straight lines (short dashs) with slope -2.5 (radiation) and -2 (matter) are included for comparison.

and

$$\mathcal{N} = \frac{2(2 - \beta)\Upsilon}{\zeta} \tag{A.17}$$

This form shows that the slope of the loop distribution at intermediate scales is completely determined by the rate of expansion: $dN/dVdl \propto l^{-2.5}$ for $n = 1/2$ and $\propto l^{-2}$ for $n = 2/3$ as previously demonstrated by Vanchurin et al. [28].

Figure 6 compares the distributions at $t = t_{today}$ and at $10^{-2}t_{today}$. The gravitational wave damping destroys the small scale loops while the expanding horizon continuously gives rise to larger scale loops. The expansion decreases the number density. The intermediate form, supplemented by the appropriate $\mathcal{G}$, will generally be sufficient to describe the loop distribution for loops that cannot have decayed ($l > l_{g,2}$ where $l_{g,2} = l_g(t_2)$) and smaller than the largest loop formed ($l < l_{max,1}$ where $l_{max,1} = \alpha_U t_1$), presuming the ordering $l_{g,2} < l < l_{max,1}$. Of course, the full expression is needed to describe the exact form near small and large l and to deal with situations in which the intermediate regime does not have enough time to form.

We are primarily interested in understanding whether various integrals are dominated by the small or large scale part of the distribution. Consider the density distribution of l^Q; $Q = 0$ gives number density, $Q = 1$ gives length (needed for energy density and lensing estimates), and so forth. Using the intermediate form for $l_{g,2} < l < l_{max,1}$

$$\int l^Q \frac{dN}{dVdl}(t_2; t_0, t_1)dl \sim \mathcal{G}\frac{\mathcal{N}\alpha_U^{2-3n}}{t_2^{3n}(Q - 3 + 3n)}\left(l_{max,1}^{Q-3+3n} - l_{g,2}^{Q-3+3n}\right) \tag{A.18}$$

Clearly, $Q < 3 - 3n$ is dominated by small scale loops ($Q < 3/2$ for $n = 1/2$; $Q < 1$ for
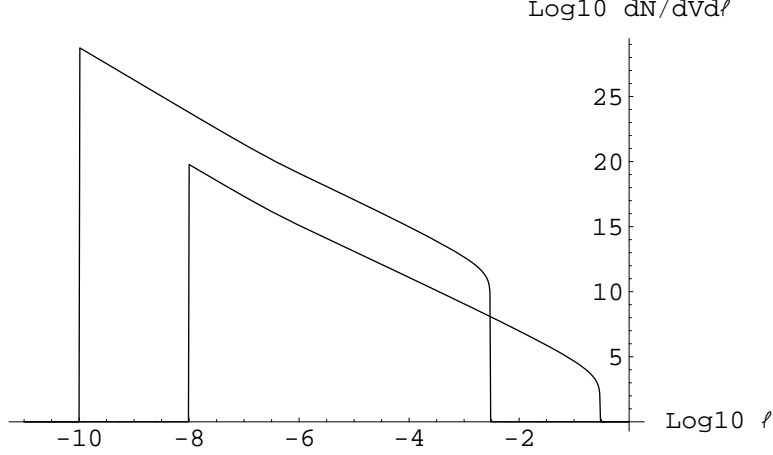
Figure 6: Number density of the string length distribution at two epochs t_{today} and $10^{-2}t_{today}$ in the two powerlaw model.

$n = 2/3$). Assuming $\alpha_U t_1 \geq \alpha_G t$ the integrations give the relatively simple forms

$$\int l \frac{dN}{dV\,dl}(t; t_0, t_1)dl \sim \mathcal{G}\frac{\mathcal{N}}{t^2} \begin{cases} 2\left(\sqrt{\frac{\alpha_U}{\alpha_G}} - \sqrt{\frac{t}{t_1}}\right) & \text{if } \text{n=1/2} \\ \log\left(\frac{\alpha_U t_1}{\alpha_G t}\right) & \text{if } \text{n=2/3} \end{cases} \tag{A.19}$$

The total integral is formed from the sum of loops created during the radiation and matter-dominated epochs ($\mathcal{G}_1 = (t_{eq}/t)^{1/2}$, $\mathcal{G}_2 = 1$). We assume (for lack of any more complete information) $\beta_1 = \beta_2$, $\alpha_{U,1} = \alpha_{U,2}$ and $\alpha_{G,1} = \alpha_{G,2}$. The final result for $t = t_{today}$ is

$$\int l \frac{dN}{dV\,dl}dl \sim \frac{1}{t^2}\left(2\mathcal{N}_1\left(\sqrt{\frac{\alpha_U t_{eq}}{\alpha_G t}} - 1\right) + \mathcal{N}_2\log\left(\frac{\alpha_U}{\alpha_G}\right)\right). \tag{A.20}$$

If $\alpha_G t_{today} \ll \alpha_U t_{eq}$ the loops created before t_{eq} dominate and

$$\int l \frac{dN}{dV\,dl}dl \to \frac{2\mathcal{N}_1}{t^2}\sqrt{\frac{\alpha_U t_{eq}}{\alpha_G t}} \tag{A.21}$$

The total energy density is

$$\rho_{loop} = \mu \int l \frac{dN}{dV\,dl}dl \tag{A.22}$$

Figure 7 plots $l^2 dN/dV\,dl$ so that contributions in different logarithmic intervals of l can be directly compared. Evidently, for the parameters adopted the small loops formed during at $t < t_e$ dominate ρ_{loop}. This result (and other qualitative results alluded to above) will be altered if $\alpha_G/\alpha_U > t_{eq}/t_{today} \sim 3.5 \times 10^{-6}$.

For a flat, matter-dominated cosmology (i.e. ignoring Λ) we find that

$$\Omega_{loop} = 6\pi G\mu\left(2\mathcal{N}_1\left(\sqrt{\frac{\alpha_U t_{eq}}{\alpha_G t}} - 1\right) + \mathcal{N}_2\log\left(\frac{\alpha_U}{\alpha_G}\right)\right). \tag{A.23}$$
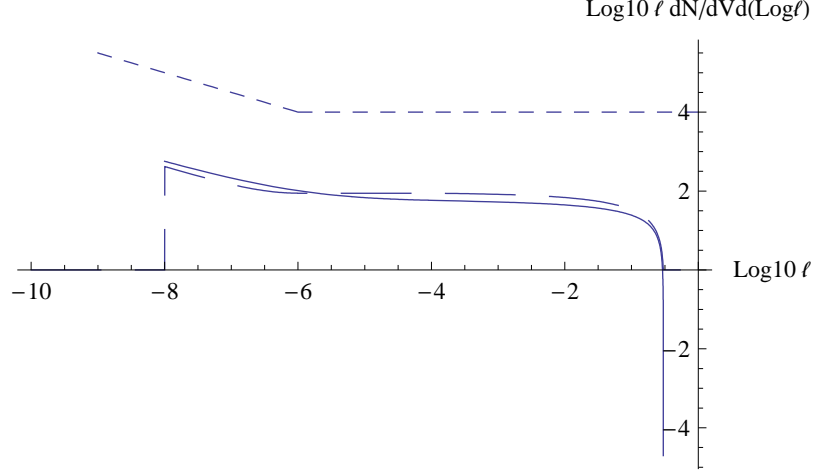
Figure 7: Today's string number distribution weighted by length; lines as in previous plot; straight (short dashed) lines have slope -.5 (radiation) and 0 (matter).

A.2 Analytic Estimate

Define two dimensionless parameters, scale to "typical" parameters, as follows:

$$X = X_0 \left(\frac{\alpha_U}{0.3}\right) \left(\frac{10^{-8}}{\Gamma_R G\mu}\right) \tag{A.24}$$

$$X_0 = 3 \times 10^7 \tag{A.25}$$

$$Y = Y_0 \left(\frac{X}{X_0}\right) \left(\frac{t_{eq}}{4.7 \times 10^4 \text{yrs}}\right) \left(\frac{1.35 \times 10^{10}\text{yrs}}{t_{today}}\right) \tag{A.26}$$

$$Y_0 = 104.4 \tag{A.27}$$

which gives

$$\int l \frac{dN}{dV dl} dl \sim \frac{1}{t^2} \left(\mathcal{N}_1 \left(20.4\sqrt{\frac{Y}{Y_0}} - 2\right) + \mathcal{N}_2 \left(17.22 + \log\left(\frac{X}{X_0}\right)\right)\right) \tag{A.28}$$

$$\mathcal{N} = \frac{2(2-\beta)\Upsilon}{\zeta\left(1 - \left(\frac{\alpha_L}{\alpha_U}\right)^{2-\beta}\right)} \tag{A.29}$$

$$\zeta = 4 - 3n - \beta \tag{A.30}$$

Adopting numerical parameters approximately consistent with the VS simulations

$$\alpha_U = 0.3 \tag{A.31}$$

$$\alpha_L = 10^{-4} \tag{A.32}$$

$$\beta = 1.6 \tag{A.33}$$

$$\Upsilon = 43.6 \tag{A.34}$$

we find

$$\mathcal{N}_1 = 40.4 \tag{A.35}$$

$$\mathcal{N}_2 = 90.9 \tag{A.36}$$

and

$$\int l \frac{dN}{dV dl} dl \sim \frac{2250}{t^2} H(X,Y) \tag{A.37}$$

$$\Omega_{loops} \sim 8.5 \times 10^{-6} \left(\frac{G\mu}{2 \times 10^{-10}} \right) H(X,Y) \tag{A.38}$$

$$H(X,Y) \sim \left(0.63 + 0.37 \sqrt{\frac{Y}{Y_0}} + 0.04 \log \left(\frac{X}{X_0} \right) \right) \tag{A.39}$$

where X and Y depend upon $\alpha_U / \Gamma_R G\mu$ and cosmological timescales.

A.3 Λ-CDM

For a more realistic cosmology, consider a Λ-CDM model. Let $\Omega_{r,0} = 8.4 \times 10^{-5}$ $\Omega_{m,0} = 0.3$ and $\Omega_{\Lambda,0} = 1 - \Omega_{r,0} - \Omega_{m,0}$. The relationship between a and t is given by

$$\int_0^a da \frac{1}{\sqrt{\Omega_{r,0} a^{-2} + \Omega_{m,0} a^{-1} + \Omega_{\Lambda,0}}} = \tau \tag{A.40}$$

where $\tau(a) = H_0 t(a)$. We choose $a = 1$ today $(t(1) = t_{today}$, $H_0 = \tau(1)/t_{today})$ or $t(a) = t_{today} \tau(a)/\tau(1)$ and $V(a) \propto a^3$. Assuming that all parameterized quantities $(\beta, \alpha_U, \alpha_L, \alpha_G, \gamma_s)$ are constant, we evaluate the loop density at t_{today} numerically

$$\frac{dN}{dV dl} = \frac{A}{l^\beta V(t_{today})} \int_{t_0^*}^{t_1^*} dt' t'^{\beta-5} V(t') \tag{A.41}$$

where

$$t_1^* = \min \left(t_{today}, \frac{l}{\alpha_L} \right) \tag{A.42}$$

$$t_0^* = \max \left(0, t_{today} - \frac{l}{\alpha_G}, \frac{l}{\alpha_U} \right). \tag{A.43}$$

These results are included on the plots; they are the solid, smooth lines. They agree fairly well with the simple, two-powerlaw approximation.

A.4 Λ-CDM: Numerical Results for varying $G\mu$, α_U, α_L and β

We choose a fiducial set of parameters: $\beta = 1.6$, $\Gamma_R G\mu = 10^{-8}$, $\alpha_U = 0.3$ and $\alpha_L = 10^{-4}$. We then varied a single parameter over a wide range to explore how the loop distribution function changed.
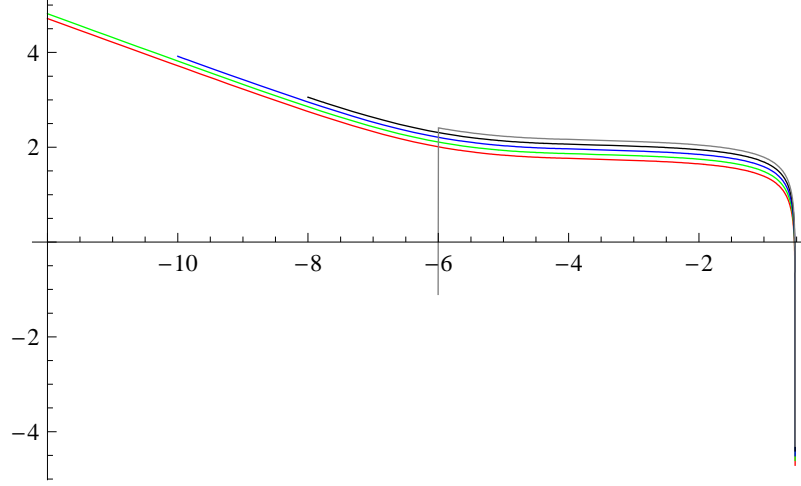
Figure 8: Loop distribution for $\Gamma_R G\mu = 10^{-15}$ to 10^{-9} in steps of 10^2 for standard case. Slight offsets to expose separate curves. Lower $\Gamma_R G\mu$ extend to smaller loop size.

Effect of variation of $G\mu$ on the loop distribution is illustrated in Figure 8. Decreasing the tension extends the distribution to smaller size scales because gravitational radiation is less rapid.

Effect of variation of β on the loop distribution is illustrated in Figure 9. Smaller β concentrates loops at the largest scale relative to the horizon. These large loops live longer with respect to gravitational wave damping modestly increasing the abundance of the smallest loops.
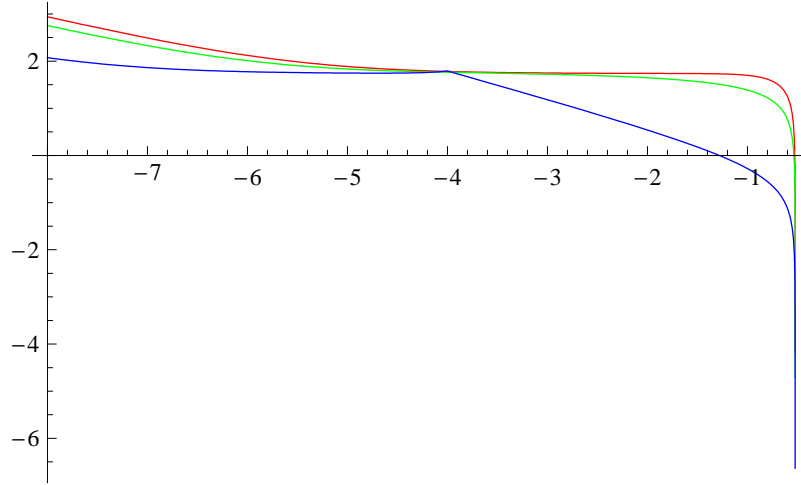

Figure 9: Loop distribution for $\beta = 0.6$ (red), 1.6 (green) and 2.6 (blue).

Effect of variation of α_U on the loop distribution is illustrated in Figure 10. Smaller α_U limits the size of the loops at all times and leads to more rapid decay.

Effect of variation of α_L on the loop distribution is illustrated in Figure 11. Larger α_L increases the size of the loops at all times and leads to less rapid decay.
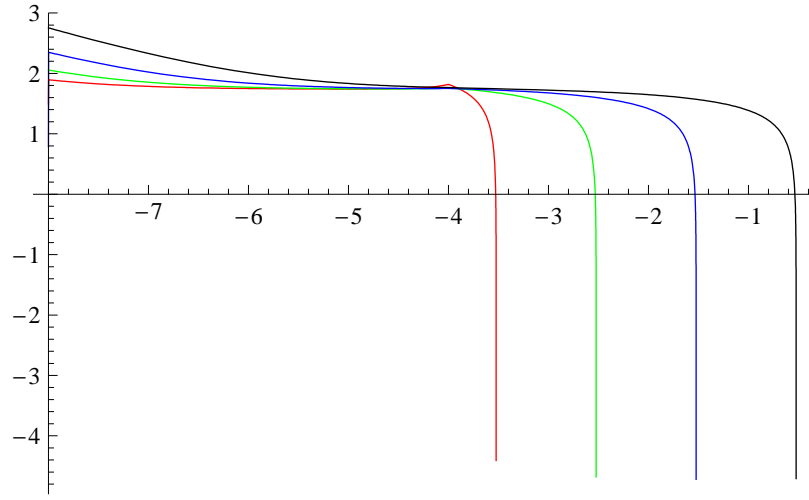
Figure 10: Loop distribution for $\alpha_U = 3 \times 10^{-4}$ (red), 3×10^{-3} (green), 3×10^{-2} (blue), 0.3 (black).
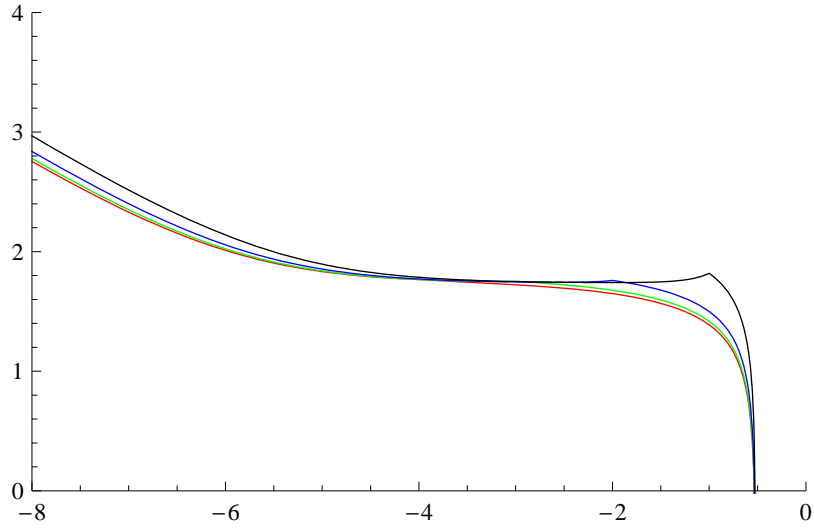

Figure 11: Loop distribution for $\alpha_L = 10^{-4}$ (red), 10^{-3} (green), 10^{-2} (blue), 0.1 (black).

References

[1] A. H. Guth, *The Inflationary Universe: A Possible Solution To The Horizon And Flatness Problems*, Phys. Rev. D **23**, 347 (1981);
A. D. Linde, A New Inflationary Universe Scenario: A Possible Solution Of The Horizon, Flatness, Homogeneity, Isotropy And Primordial Monopole Problems, Phys. Lett. B **108**, 389 (1982);
A. Albrecht and P. J. Steinhardt, *Cosmology For Grand Unified Theories With Radiatively Induced Symmetry Breaking*, Phys. Rev. Lett. **48**, 1220 (1982).

[2] G. R. Dvali and S.-H. H. Tye, *Brane inflation*, Phys. Lett. B **450**, 72 (1999), hep-ph/9812483.

[3] C. P. Burgess, M. Majumdar, D. Nolte, F. Quevedo, G. Rajesh and R. J. Zhang, *The inflationary brane-antibrane universe*, JHEP **0107**, 047 (2001), hep-th/0105204;
G. R. Dvali, Q. Shafi and S. Solganik, *D-brane inflation*, hep-th/0105203.

[4] S. Kachru, R. Kallosh, A. Linde, J. Maldacena, L. McAllister and S. P. Trivedi, *Towards inflation in string theory*, JCAP **0310** (2003) 013, hep-th/0308055.

[5] N. Jones, H. Stoica and S.-H. H. Tye, *Brane interaction as the origin of inflation*, JHEP **0207**, 051 (2002), hep-th/0203163.

[6] S. Sarangi and S.-H. H. Tye, *Cosmic string production towards the end of brane inflation*, Phys. Lett. B **536**, 185 (2002), hep-th/0204074.

[7] G. Dvali and A. Vilenkin, *Formation and evolution of cosmic D-strings*, JCAP **0403**, 010 (2004), hep-th/0312004.

[8] E. J. Copeland, R. C. Myers and J. Polchinski, *Cosmic F- and D-strings*, JHEP **0406**, 013 (2004), hep-th/0312067.

[9] H. Firouzjahi, L. Leblond and S. H. Henry Tye, *The (p,q) string tension in a warped deformed conifold*, JHEP **0605**, 047 (2006), hep-th/0603161.

[10] S. H. H. Tye, *Brane inflation: String theory viewed from the cosmos*, hep-th/0610221.

[11] J. Polchinski, *Cosmic String Loops and Gravitational Radiation*, arXiv:0707.0888 [astro-ph].

[12] A. Vilenkin and E.P.S. Shellard, Cosmic strings and other topological defects, Cambridge University Press, 2000.

[13] X. Chen and S.-H. H. Tye, *Heating in brane inflation and hidden dark matter*, JCAP **0606**, 011 (2006), hep-th/0602136.

[14] M. Landriau and E. P. S. Shellard, *Large angle CMB fluctuations from cosmic strings with a cosmological constant*, Phys. Rev. D **69** 023003 (2004), astro-ph/0302166;

L. Pogosian, M. Wyman and I. Wasserman, *Observational constraints on cosmic strings: Bayesian analysis in a three dimensional parameter space*, JCAP 09 (2004) 008, astro-ph/0403268; *Bounds on cosmic strings from WMAP and SDSS*, astro-ph/0503364; E. Jeong and G. F. Smoot, *Search for cosmic strings in CMB anisotropies*, astro-ph/0406432; P. Wu, *Coherence Constraint on the Existence of Cosmic Defects*, astro-ph/0501239.

[15] F. A. Jenet *et al.*, *Upper bounds on the low-frequency stochastic gravitational wave background from pulsar timing observations: Current limits and future prospects*, Astrophys. J. **653**, 1571 (2006) [arXiv:astro-ph/0609013].

[16] X. Siemens, V. Mandic and J. Creighton, *Gravitational wave stochastic background from cosmic (super)strings*, Phys. Rev. Lett. **98**, 111101 (2007) [arXiv:astro-ph/0610920].

[17] K. Kuijken, X. Siemens and T. Vachaspati, *Microlensing by Cosmic Strings*, arXiv:0707.2971 [astro-ph].

[18] A. Albrecht and N. Turok, *Evolution Of Cosmic Strings*, Phys. Rev. Lett. **54**, 1868 (1985); D. P. Bennett and F. R. Bouchet, *Evidence For A Scaling Solution In Cosmic String Evolution*, Phys. Rev. Lett. **60**, 257 (1988); B. Allen and E. P. S. Shellard, *Cosmic String Evolution: A Numerical Simulation*, Phys. Rev. Lett. **64**, 119 (1990).

[19] M. G. Jackson, N. T. Jones and J. Polchinski, *Collisions of cosmic F- and D-strings*, hep-th/0405229.

[20] S.-H. H. Tye, I. Wasserman and M. Wyman, *Scaling of multi-tension cosmic superstring networks*, astro-ph/0503506.

[21] K. D. Olum and A. Vilenkin, *Reionization from cosmic string loops*, Phys. Rev. D **74**, 063516 (2006) [arXiv:astro-ph/0605465].

[22] L. Eyer and F. Mignard, *Rate of correct detection of periodic signals with the Gaia Satellite*, MNRAS 361, 1136 (2005); C. Jordi et al., *The design and performance of the Gaia photometric system*, MNRAS 367, 290 (2006); L. Eyer, *Astronomical databases, Space photometry and time series analyses: Open questions*, astro-ph/05114581. L. Eyer and J. Cuypers, *Predictions on the number of variable stars for the GAIA space mission and for surveys as the ground-based International Liquid Mirror Telescope*, Symposium IAU 176, Budapest (Hungary), ASP Conference Series 203, 71 (1999)

[23] V. Vanchurin, K. Olum and A. Vilenkin, *Cosmic string scaling in flat space*, Phys. Rev. D **72**, 063514 (2005), gr-qc/0501040.

[24] C. J. A. P. Martins and E. P. S. Shellard, *Fractal Properties and small-scale structure of cosmic string networks*, Phys. Rev. D **73** 043515 (2006), astro-ph/0511792.

[25] C. Ringeval, M. Sakellariadou and F.R. Bouchet, *Cosmological evolution of cosmic string loops*, astro-ph/051164.

[26] X. Siemens and K. D. Olum, *Gravitational radiation and the small-scale structure of cosmic strings*, Nucl. Phys. B. **611**, 125 (2001), gr-qc/0104085

[27] X. Siemens, K. D. Olum and A. Vilenkin, *On the size of the smallest scales in cosmic string networks*, Phys. Rev. D**66** 043501 (2002), gr-qc/0203006

[28] V. Vanchurin, K. D. Olum and A. Vilenkin, *Scaling of cosmic string loops*, gr-qc/0511159.

[29] J. Polchinski and J. V. Rocha, *Analytic study of small scale structure on cosmic strings*, hep-ph/0606205.

[30] A. Avgoustidis and E. P. S. Shellard, *Effect of reconnection probability on cosmic (super)string network density*, Phys. Rev. D **73**, 041301 (2006) [arXiv:astro-ph/0512582].

[31] A. Vilenkin, *Cosmic strings as gravitational lenses*, Ap. J. **282**, L51 (1984).

[32] C. Hogan and R. Narayan, *Gravitational lensing by cosmic strings*, M.N.R.A.S. **211**, 575 (1984).

[33] M. Fich and S. Tremaine, *The mass of the galaxy*, Annu. Rev. Astron. Astrophys. **29**, 409 (1991).

[34] J. Binney and S. Tremaine, *Galactic dynamics*, Princeton University Press (New Jersey), 428 (1987).

[35] A. Albrecht and N. Turok, *Evolution of cosmic string networks*, Phys. Rev. D. **40**, 973 (1989).